A Robust 3D Finite Element Simulation of Human Proximal Femur Progressive Fracture Under Stance Load with Experimental Validation

RIDHA HAMBLI and SAMIR ALLAOUI

Prisme Institute, MMH, 8, Rue Leonard de Vinci, 45072, Orleans Cedex 2, France

Associate Editor Joel D. Stitzel oversaw the review of this article.

Abstract—Clinical implementation of quantitative computed tomography-based finite element analysis (QCT/FEA) of proximal femur (hip) fractures requires (i) to develop a bone material behavior able to describe the progressive fracturing process until complete failure of the hip. And (ii) to validate the model with realistic test data that represent typical hip fractures. The objective of the current study was to develop and experimentally validate an accurate 3D finite element (FE) model coupled to a quasi-brittle damage law to simulate human proximal femur fracture considering the initiation and progressive propagation of multiple cracks phases under quasi-static load. The model is based on continuum damage mechanics that can predict hip fracture in more adequate physical terms than criteria-based fracture models. In order to validate the model, ten human proximal femurs were tested until complete fracture under one-legged stance quasi-static load. QCT/FE models were generated and FE simulations were performed on these femurs with the same applied loads and boundary conditions than in the stance experiments. The proposed FE model leads to excellent agreement ($R^2 = 0.9432$) between predicted and measured results concerning the shape of the force–displacement curve (yielding and fracturing) and the profile of the fractured edge. The motivation of this work was to propose a FE model for possible clinical use with a good compromise between complexity and capability of the simulation.

Keywords—Proximal femur, Fracture, Finite element, Experimental validation, Fracture pattern, Force–displacement curve.

INTRODUCTION

The bones of elderly people with osteoporosis are susceptible to traumatic fracture as a result of external impact. Modeling the fracture behavior of bone tissue will help researchers find proper treatments to strengthen the bone in order to prevent such fractures.

Finite element (FE) analysis has proven to be a useful method for studying the mechanical characteristics of hip fracture. CT-based nonlinear FE analysis that incorporates three-dimensional geometry and bone density distribution has been shown to be a useful method to predict hip fracture under given boundary conditions (stance, side fall,…) with reasonable accuracy.[12] However, simple and practical validated FE models with a good compromise between complexity and accuracy of the simulation considering a limited number of model parameters are still needed for possible clinical use.

Quantitative computed tomography (QCT) provides 3D FE models considering the three-dimensional (3D) proximal femur geometry and bone density distribution. Several QCT/FE models were proposed in the past.[18,36,38,43,58]

Previous QCT/FE models have applied different uncoupled fracture criteria including von Mises equivalent stress, equivalent stress, maximum principal strain criterion Hill's criterion and Drucker–Prager criterion in order to predict the onset of human proximal femur fracture under excessive load. Such criteria are limited in general to the prediction of the initiation of local bone failure only. They do not take into consideration the complete fracturing process of proximal femur and the loss of bone material stiffness generated by progressive damage accumulation prior to fracture. Recently, several authors investigated the fracture of cortical bone based on fracture mechanics concepts[2,44,61,65,66] but failed to predict the complete fracture pattern of bone since these methods are restricted to the problem of a single dominant idealized planar crack. Recently, FE models based on continuum damage mechanics (CDM) were developed to

Address correspondence to Ridha Hambli, Prisme Institute, MMH, 8, Rue Leonard de Vinci, 45072, Orleans Cedex 2, France. Electronic mail: ridha0007@yahoo.com, ridha.hambli@univ-orleans.fr

simulate human bone fracture.[15,21–23] In spite of the large number of FE studies dealing with bone fracture under monotonic load there is still a lack of practical and simple validated FE models that simulate the complete bone failure and predict realistic and accurate force–displacement (F/U) curves and fracture patterns.[12]

Several studies showed that bone exhibits a quasi-brittle material behavior[5,14,29,30,39,55] or brittle behavior[28,42,57,69] depending mainly on the deformation rate applied and the bone properties. Therefore, more physical hip fracture FE models can be developed by incorporating the CDM concept in order to predict the progressive initiation and propagation of cracks, leading to complete fracture of the bone.

In the present work, an isotropic 3D QCT/FE model coupled to a quasi-brittle damage law was developed in order to simulate fracture of human proximal femurs under quasi-static load and predict the complete F/U curve and the final fracture pattern of the proximal femur under one-legged stance load. The element deletion technique was applied in order to simulate the progressive fracturing process of bone.[23]

The use of a CDM is useful to describe fracture propagation in a continuous-like material. However, bone is a hierarchically organized material at different length scales.[40] Each element of the hierarchy has different stiffness and strength and the overall Young modulus and ultimate strength results from the hierarchic combination of these levels.[19,24,27] The complexity and heterogeneity of bone tissue require a multiscale modeling to understand its mechanical behavior.

Many researchers have recently developed analytical or numerical models to describe the multiscale behavior of bone fracture.[7,19,21,22] These models use homogenization techniques and provide bone material parameters averaged at macroscopic continuum scale.

Bone resists fracture through several mechanisms depending on hierarchical scale ranging from fracture of mineralized tropocollagen to whole organ fracture.[71] It has been reported these fracturing processes depend on (i) intrinsic mechanisms that promote plasticity at small length scales and (ii) extrinsic mechanisms that shield the growing crack at larger length scales.[71] At lower scale mineralized collagen fibril and the secondary osteon at the microstructural level play main roles on the bone cracking resistance.[71] At higher length he osteon has a central vascular cavity that is concentrically surrounded by sheets of lamellae.[46] At its outer boundary, the secondary osteon contains an interface (cement line), which represents an weak region acting as a site where major microcracks form and its alignment with the long axis of the long bones is the primary cause of the anisotropic toughness of cortical bone. It is through this hierarchical structure that human cortical bone is able to develop its unique combination of strength and toughness.[46]

The current CDM isotropic strategy is motivated by: (i) performing fracture FE simulations of a whole bone organ considering its multiscale structure is very complicated and requires a tremendous computation time. (ii) Some published comparative studies claiming that the assigned orthotropic material model has a limited effect on the FE result at bone compared to the isotropic one,[4,53,67] and (iii) the complexity regarding the assignment of the local anisotropic directions for every FE of the mesh and their corresponding anisotropic material properties.[56,62]

In order to validate the model, ten human proximal femurs were tested until complete fracture under one-legged stance quasi-static load. QCT/FE models were generated and FE simulations were performed on these femurs with the same applied loads and boundary conditions than in the stance experiments.

The stance configuration has been shown in previous studies to produce maximum shear stresses in the femoral neck region in a manner consistent with clinical subcapital fractures[10,59] similar to the predicted one.

The predicted F/U curves and the fracture patterns were compared for the ten specimens. The calibration of the method was performed in a set of three of the ten specimens, and validated on the remaining seven specimens. The numerical calibration phase was used to establish the relationship between the FE density and the strain at fracture needed for the damage growth description.

Excellent agreement ($R^2 = 0.9432$) were obtained between predicted and measured results which indicate that the proposed FE proximal femur fracture model in the quasi-static regime can capture the initiation and propagation of the cracks within the femurs until complete failure of the bone.

MATERIALS AND METHODS

Femur Samples

Ten human cadaveric femurs (seven females and three males) were provided by the Institute of Anatomy (University of Paris V, Paris, France). Individuals with bone diseases other than osteoporosis or osteopenia were excluded from the study.

Freshly drawn femurs were wrapped between all processing steps in a cloth soaked in saline (NaCl 0.9%) in order to avoid dehydration. All samples were defatted softly, without causing any damage to the bone, by submerging each of them two hours in hot bleach at 85 °C. This operation was repeated twice for each specimen after cooling between two stages. The

samples were stored in a refrigerator at a temperature of 4 °C.

The characteristics of the selected femurs are presented in Table 1.

QCT Scanning

Each femur specimen was scanned perpendicular to the diaphyseal main axis. The CT-scan acquisition started 1 cm above the femoral head and ended at about 30 mm distal to the lesser trochanter, requiring a total scan length of approximately 150 mm.

The CT-scan slices were obtained using a multislice device (Somatom Plus 4 Volume Zoom, Siemens, Erlangen, Germany) at the following acquisition and reconstruction parameters: 120 kVp, 160 mAs, image matrix 512×512 pixels, and field of view of 150×150 mm. A high-resolution protocol with a slice thickness of 0.7 mm was used with an in-plane spatial resolution approximately 0.25 mm $\times$ 0.25 mm.

Images were obtained in Digital Imaging and Communications in Medicine (DICOM) format for segmentation and analysis.

Each of the voxels defined by the QCT scan gives the Hounsfield Unit (HU), which can be correlated to the local density resulting in an inhomogeneous distribution, from which Young's modulus and strain at fracture were computed.

Each CT dataset was calibrated using a Phantom (Osteo, Siemens, Erlangen, Germany) constituted of a water equivalent plastic component and a bone-equivalent plastic component (200 mg calcium hydroxyapatite per milliliter) for individual conversion of HU to equivalent mineral density ρ_{EQM}. The following calibrated relation was established ($R^2 = 0.9987$):

$$\rho_{EQM} = 6.932 \times 10^{-4} \times HU - 5.68 \times 10^{-4} \, (\text{g/cm}^3) \tag{1}$$

The ash density is expressed by Keyak and Falkinstein[33]:

$$\rho_{ash} = 1.22 \, \rho_{EQM} + 0.0523 \, (\text{g/cm}^3) \tag{2}$$

Stance Configuration Fracture Testing

After acquisition, the 10 human proximal femurs were prepared for mechanical testing until complete fracture, under a one-legged stance quasi-static load. The femurs were fixed on the experimental apparatus designed and built for this purpose. The distal portion of each femur was fixed on the holder with epoxy resin (SICOMIN Epoxy Systems, France). Once the resin had been cured, the human femurs were installed in the single limb set up (Fig. 1). The holder maintained the orientation of the bone such that the neck was internally rotated 20° within the coronal plane following previous studies performed on proximal femurs.[6,33,51] Each proximal femur was placed in INSTRON testing machine (model 4411, Instron Corp., canton, USA) and quasi-static compressive loads were applied from zero until complete fracture of the specimens with an increased force of 50 N steps (Fig. 1) at a constant low loading speed equal to 20 mm min^{-1}.

Finite Element Modeling

In the quasi-static regime, the isotropic stress–strain relation of elasticity based damage mechanics is expressed by Hambli[23,25] and Lemaitre[41]:

$$\sigma_{ij} = (1 - D)C_{ijkl}\varepsilon_{kl} \tag{3}$$

where D denotes the damage variable, σ_{ij} the stress components, ε_{kl} the strains and C_{ijkl} are the elasticity tensor components.

The amount of micro-damage in an experimental specimen has been positively correlated with applied post-yield strain following a power law relationship.[3,50] Based on these results, an experimentally relevant damage law can be expressed in the general normalized form:

TABLE 1. Femur samples characteristics.

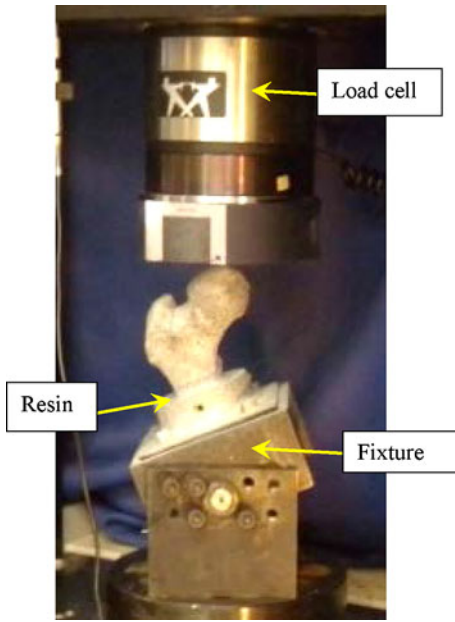| Specimen	Donor age	Gender	Side	Neck aBMD (g/cm^2)	Total aBMD (g/cm^2)
A	85	F	Right	0.41	0.64
B			Left	0.45	0.72
C	91	F	Right	0.50	0.75
D			Left	0.48	0.68
E	80	M	Right	0.75	0.83
F			Left	0.79	0.86
G	98	F	Left	0.49	0.62
H	100	F	Left	0.43	0.53
I	62	M	Left	0.74	0.99
J	87	F	Left	0.51	0.68

FIGURE 1. Experimental set-up for the proximal femur specimens' tests.

$$\begin{cases} D = 0; & \varepsilon_{eq} \leq \varepsilon_y \\ D = D_c \left(\dfrac{\varepsilon_{eq}}{\varepsilon_y} \right)^n; & \varepsilon_y < \varepsilon_{eq} < \varepsilon_f \\ D = D_c; & \varepsilon_{eq} \geq \varepsilon_f \end{cases} \quad (4)$$

ε_{eq}, D_c, n, ε_y, and ε_f are respectively the equivalent strain, the critical damage at fracture, the damage exponent, yield strain (damage strain threshold when damage starts) and the strain at fracture.

The equivalent strain ε_{eq} is expressed by:

$$\varepsilon_{eq} = \sqrt{\frac{2}{3} \varepsilon_{ij} \varepsilon_{ij}} \quad (5)$$

ε_{ij} are the strain tensor components.

Mesh Dependence Regularization to Damage

In the constitutive law of conventional CDM there is no intrinsic material characteristic length, which means that crack propagation results are dependent on the mesh size.[49]

An alternative and simple method to ensure the objectivity of the numerical model in relation with the physical cracking process and the mesh dependence problem consists in weighting (linear form) the strain at fracture (ε_f) as a function of a characteristic FE length (L_{FE}) and the crack length (L_{frx}) in the form (Abaqus 6.11)[1]:

$$\varepsilon_f^T = \varepsilon_{f-true}^T \left(\frac{L_{frx}}{L_{FE}} \right) \quad (6a)$$

$$\varepsilon_f^C = \varepsilon_{f-true}^C \left(\frac{L_{frx}}{L_{FE}} \right) \quad (6b)$$

where ε_{f-true}^T and ε_{f-true}^C denote respectively, the true bone material measured strain at fracture in tension and compression.

L_{FE} is computed automatically and provided by Abaqus code (Abaqus 6.11) at every numerical iteration. In addition, average crack lengths found in bones are typically about 50 to 100 microns.[8,60,61] Therefore, the characteristic length L_{frx} was set to ($L_{frx} = 0.075$ mm).

The proposed mesh-dependency regularization method is recommended by the Abaqus code for crack propagation problems to ensure non-dependency of the fracture results on the FE mesh.

In addition, it has been reported that strain at fracture is bone-site dependent and exhibits a power law relationship vs. bone mineral density (BMD).[18,64] Therefore, to perform personalized prediction of a given patient, yield strain (ε_f^{true}) can be expressed vs. the bone density in the form:

$$\varepsilon_f^{true-C} = a_c \rho_{ash}^{mc} \quad \text{in compression} \quad (7a)$$

$$\varepsilon_f^{true-T} = a_t \, \rho_{ash}^{mt} \quad \text{in tension} \quad (7b)$$

a_c, a_t, mc, and mt are material parameters which can be assessed by experiments or numerical calibration procedures.

Crack Propagation Simulation

When the damage parameter reaches its critical value D_c inside an element of the mesh, its stiffness matrix is set to zero leading to the redistribution of the stress state in the vicinity of the damaged zone.[41] The propagation of the damage through the specimens is simulated by the accumulation of the completely damaged elements of the mesh during the loading. These concepts are illustrated by Fig. 2 in which the propagation of cracks is illustrated.

In CDM, there is no difference between crack initiation and propagation. Both of them result from the failure of an element of the mesh. Thus, crack initiation and propagation are studied in a unified approach.[9,23,41,48] The technique developed here distinguishes between tension, shearing and compression loading modes as follows[21,22,52]:

$$D_c = 0.95 \quad \text{In tension}$$
$$D_c = 0.95 \quad \text{In compression and shearing}$$

FE Mesh Generation

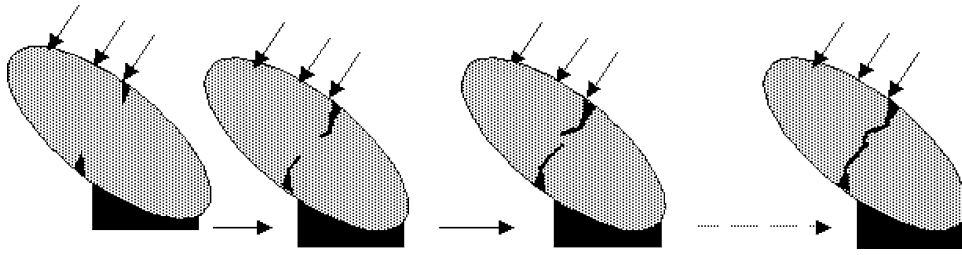In the present case, the 3D FE models were generated in a semi-automatic way from the DICOM files of

FIGURE 2. Illustration of damage initiation and propagation concept (damaged elements are presented in black).

the femurs to obtain a set of slices by QCT using an in-house software (Fig. 3). Previous studies that investigated the model convergence recommended using an element size of ≤3 mm to accurately capture the heterogeneous variations in the mechanical properties[6,37,38] and to ensure a precise prediction of the fracture path growth.[23] To investigate the mesh convergence problem and the regularization approach related to damage growth mesh-dependence problem, each femur was meshed with three different characteristic element lengths (L_{FE}) that are designated as coarse (L_{FE} = 3 mm), medium (L_{FE} = 2 mm) and fine (L_{FE} = 1 mm). First, the contours of the femur were extracted from the CT scan. Based on these contours, the surface of the bone was reconstructed, from which, in a second step, FE meshes with about 20,000 to 155,000 tetrahedral elements were generated. The F/U curves and fracture patterns were computed and compared for all the specimens.

We applied the same loads and boundary conditions than in the previously described experiments.

Assignment of Material Properties

Several empirical relationships between Young's modulus and bone ash density were proposed in the published literature. In the current work, we used the Keyak and Falkinstein relation[33] which was shown to provide the closest results when compared to *in vitro* experiments[63] to assign the Young's modulus for the human femur specimens:

$$E = 33,900\rho_{ash}^{2.20} \text{ for } \rho_{ash} \leq 0.27 \quad (8a)$$

$$E = 5307\rho_{ash} + 469 \text{ for } 0.27 < \rho_{ash} < 0.6 \quad (8b)$$

$$E = 10,200\rho_{ash}^{2.01} \text{ for } \rho_{ash} \geq 0.6 \quad (8c)$$

The Poisson's ratio is kept constant $v = 0.3$.

A calibration of the method was performed in a set of three of the ten specimens consisting in performing parametric FE simulations with several model parameters to obtain optimal mapping of projection density values to strain at fracture (Eqs. (Eqs. 7a, 7b) using optimal parameter identification based on a trial and error optimization procedure. An in-house optimization procedure based on Gauss–Newton search algorithm developed in Python and coupled with Abaqus code were applied during these simulations in order to minimize the error between the predicted F/U curve and the experimentally recorded.[20] Finally, we found that the best fit is given by a yield strain (ε_f^{true}) relationship expressed by:

Cortical bone:

$$\varepsilon_f^{true-C} = 0.0854\rho_{ash}^{-0.19} \text{ in compression} \quad (9a)$$

$$\varepsilon_f^{true-T} = 0.00575\,\rho_{ash}^{-0.21} \text{ in tension} \quad (9b)$$

Trabecular bone:

$$\varepsilon_f^{true-C} = 0.0218\,\rho_{ash}^{0.43} \text{ in compression} \quad (9c)$$

$$\varepsilon_f^{true-T} = 0.00867\,\rho_{ash}^{0.45} \text{ in tension} \quad (9d)$$

Equations (9a)–(9d) were then used in the FE fracture simulations for the 7 remaining femurs of the validation set.

Sensitivity Analysis to Critical Damage at Fracture

Because of uncertainty concerning the critical damage at fracture parameters (D_c^T and D_c^C), a sensitivity analysis (SA) was performed to investigate the impact of the sensitivity of these factors on the femur fracture force. In the current work, a limited preliminary one-factor SA analysis was performed where only one model parameter (D_c^T or D_c^C) value was varied by a given percent (Table 2) while the other parameter were kept at their reference values. For each parameter change, a fracture simulation was performed for every specimen and the proximal femur fracture force was computed. SA analysis consists of 120 runs (12 cases × 10 femurs) for every critical damage parameter change (Table 2).

RESULTS

A mesh convergence analysis of a representative femur (specimen G) (Fig. 4) was performed for three different mesh sizes (coarse, medium and fine). The
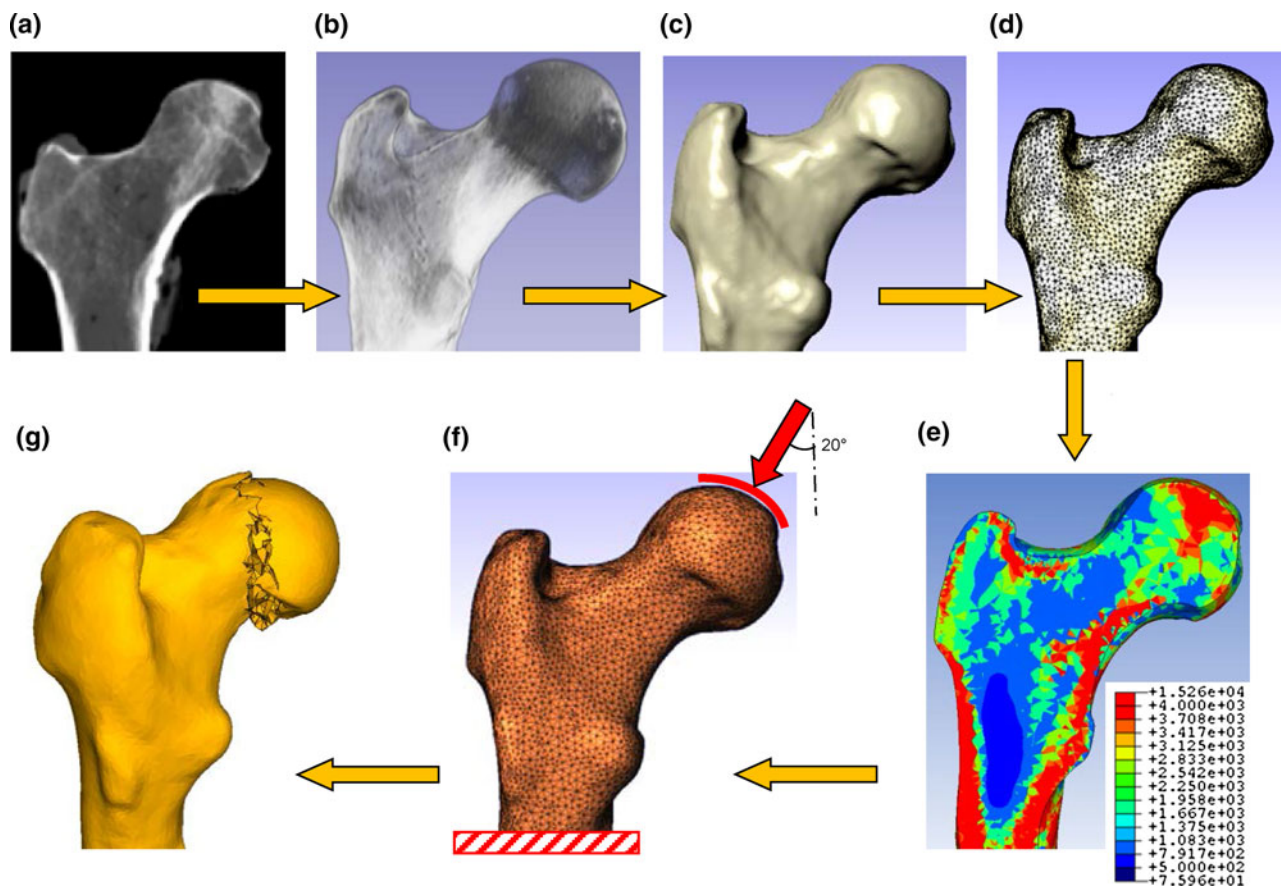
FIGURE 3. Overview of FE model generation: (a) QCT scan of a femur (specimen G). (b) Model segmentation. (c) FE model. (d) FE mesh using parabolic tetrahedral elements. (e) A cross section showing the heterogeneous material properties assignment (Young modulus and strain at fracture). (f) Application of boundary conditions consisting in: (i) application of nodal displacements of a set of selected nodes located at top surface of the femur head (red line) with an orientation of 20° from the shaft axis until complete fracture and (ii) the distal portion of the model was restrained. Movement perpendicular to the applied displacements was permitted. (g) Prediction of fracture pattern.

TABLE 2. Six selected values of critical damage at fracture to investigate the model sensitivity on the predicted mechanical response.

	Value 1	Value 2	Value 3	Value 4	Value 5	Value 6
Critical damage at fracture in tension: D_c^T	0.95 (Reference)	0.76	0.8	0.855	0.9	1
Critical damage at fracture in compression: D_c^C	0.5 (Reference)	0.4	0.45	0.55	0.6	0.65
Force at fracture (kN)	8.2	6.55	7.4	8,77	9.18	11.2

D_c^T were varied with −20, −15, −10, −5, 0 and +5% (D_c^C kept equal to 0.5) and D_c^C were varied with −20, −10, 0, +10, +20 and +30% (D_c^T kept equal to 0.95).

convergence indicators retained here are the shape of the predicted F/U curves (Fig. 4a) and the fracture patterns (Fig. 4b).

Predicted results indicated that the models were fully converged at element size < 3 mm. Little difference can be observed concerning the F/U curves during the post fracture behavior with a maximum fracture force error less than 2%. Nevertheless, for fine mesh, a rapid drop of the curve after the occurrence of the first cracks indicates that fine meshes could lead to an increase of the softening rate during the fracturing

process (cracks propagation speed increases with the mesh refinement). These results reveal that very limited mesh dependence remains during the damage propagation stage. Nevertheless, this limited effect has no influence on the predicted apparent ultimate stress and strain at fracture (maximum of the curve and onset of the fracture are not changed). In addition, it can be observed that the fine mesh generated a more localized fractured region compared to coarse one.

Taken together, the mesh dependency analysis showed that the overall fracture behavior of the
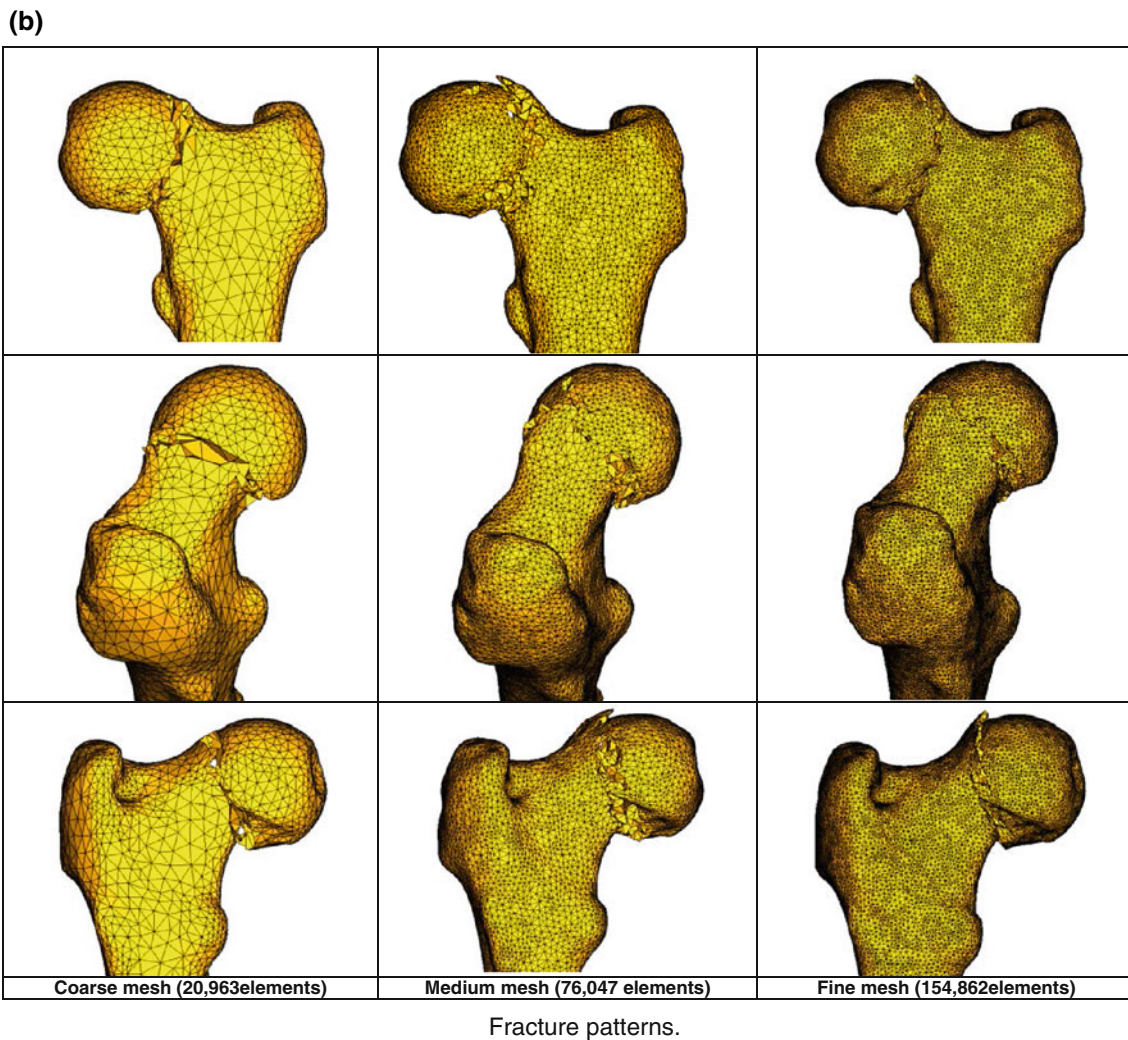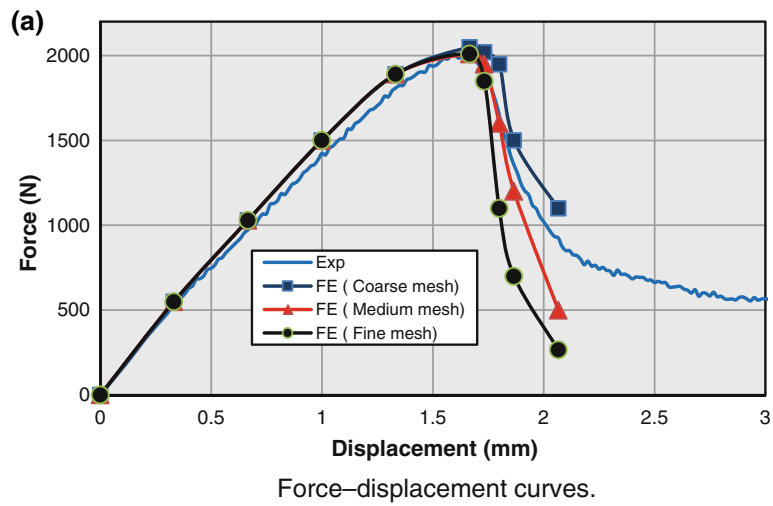
(a)

Force–displacement curves.

(b)

| Coarse mesh (20,963elements) | Medium mesh (76,047 elements) | Fine mesh (154,862elements) |

Fracture patterns.

FIGURE 4. (a) Predicted F/U curves for specimen G for three different meshes (coarse, medium and fine). (b) Predicted fracture patterns obtained by coarse, medium and fine meshes from different angles.

trabecular bone samples was very little affected by mesh size suggesting that the proposed mesh regularization technique is reliable.

Typical experimental F/U curves of three tested specimens are given in Fig. 5. The calculation time for a femur was about 20 min using a 8 Gb computer.

The predicted curves in the present study for all specimens showed the same trend for curve shape and onset of yielding and fracture as the measured experimental one. The FE-based curves exhibited a linear increase until bone yielding followed by a nonlinear behavior and drop in force during failure that was observed during all mechanical testing.

The current FE proximal femur fracture model provided excellent agreement between predicted and experimentally measured ultimate force at fracture with a correlation for the entire data set ($R^2 = 0.9432$) as shown in Fig. 6.

An example of the experimental and predicted fracture sequences of a femur (G) is given in Fig. 7.

In the yielding stage (b), the crack is initiated locally at the superior cortex located at the maximum shearing strain generated by the gradient displacement between the femur head and the subcapital region. After the yielding phase, the crack continues to grow rapidly, following a perpendicular path to the superior cortex (*c to d*). A second crack initiates at the inferior cortex which corresponds to a local combined maximum shear stress superimposed on the compressive stress generated by the applied vertical displacement and leading to complete separation of the proximal femur (*e*).
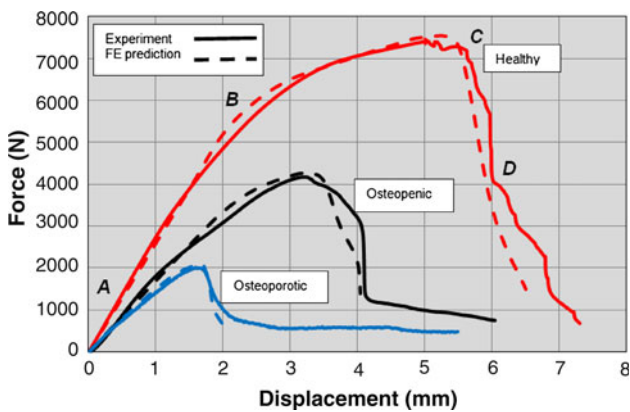

FIGURE 5. Predicted and experimental F/U curves of three specimens. Point *B* indicates the occurrence of yielding. Point *C* indicates the occurrence of numerical fracture. From *C* to *D*, the cracks propagate rapidly, leading to the drop of the curve (complete fracture of the femur).
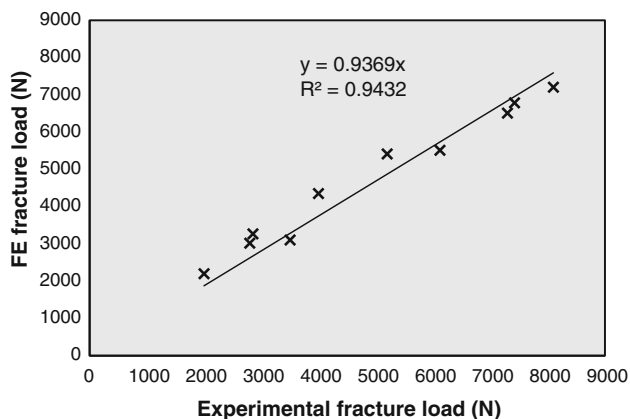

FIGURE 6. Correlation between measured and predicted ultimate force at fracture for the ten specimens.
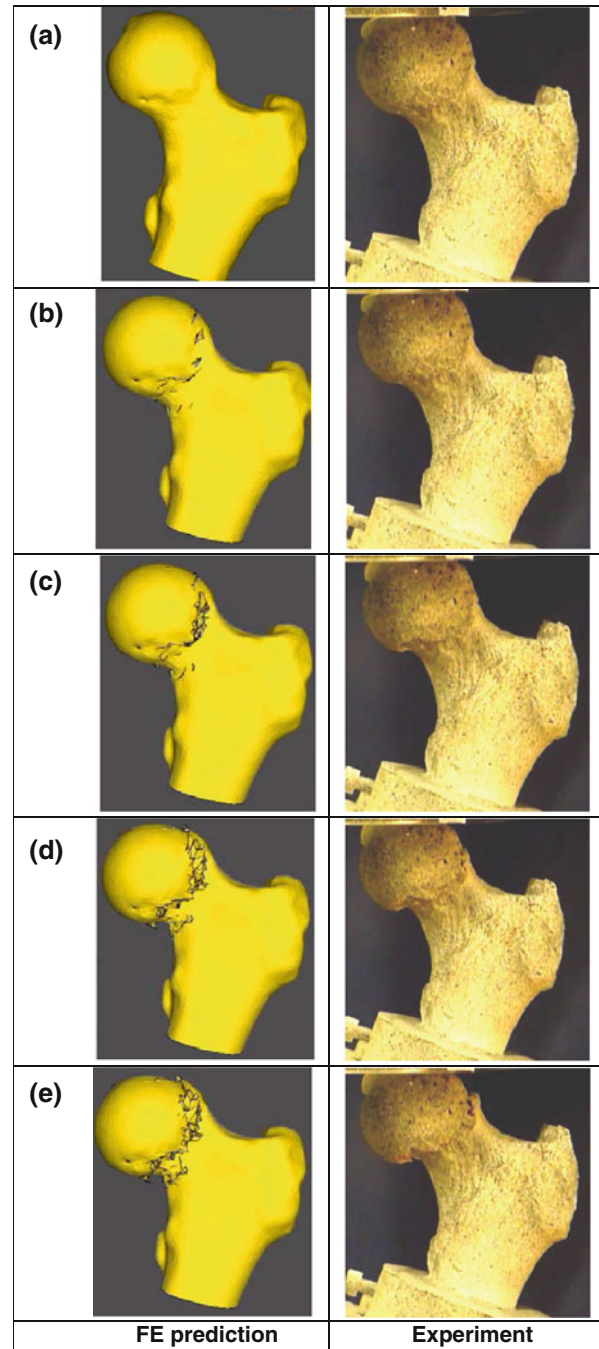

FIGURE 7. Predicted and experimentally measured crack propagation sequences within the femur for different head vertical displacements (specimen G).

An example of the experimental and predicted complete fracture patterns of two femurs with two different fracture patterns is given in Fig. 8.

For a given femur, the predicted fracture pattern corresponds to the path of the cracks after total separation of the fractured FEs of the mesh. For example, we predicted a fracture pattern with an oblique line with an angle to the horizontal plane greater than 60° (Pauwels type III) for specimens E and a subcapital fracture for specimen G. The results reveal that excellent agreement is obtained between predicted and experimental fracture patterns indicating that current CDM based FE model could be applied as a diagnostic tool in clinical applications that can detect osteoporotic fracture for aged patients in an early stage and predict bone strength accurately in individual patients.

Sensitivity Analysis

The results obtained from the SA analysis simulations are plotted in Fig. 9.

The results revealed that the variation of the critical damage generates a maximum variation of the fracture force of about 20%. Increase of the critical damage leads to increase of the fracture force. This can be related to the fact that the critical damage value plays a main role on the onset of crack initiation and propagation within bone tissue. Lower values of critical damage lead to an early cracking process and then to a decreased force at fracture. On the other hand, an increase of these parameters generates an increased resistance to fracture and therefore an increase of the fracture force. Predicted results revealed that the fracture patterns were very similar, not being significantly affected by the variation of parameters. Nevertheless, the rate of crack propagation increased with decreasing critical damage suggesting that bone fracture may range from quasi-brittle to brittle patterns depending on its material properties.

DISCUSSION

Predicted F/U curve shows a same trend as observed experimental ones concerning the curve shape and onset of the yielding and fracture.[32] The curves shows a linear phase followed by a nonlinear behavior post yielding caused by damage initiation and growth which can be shorter or longer depending mainly on bone geometry, intrinsic properties, viscosity, specimen preparation (fresh frozen, embalmed), aging (decrease of toughness of bone) and the load testing speed. The damaging phase is followed by a sharp drop in force during failure that was nearly always seen during mechanical testing (Fig. 5).

Schileo et al.[57] loaded proximal femurs in single-leg stance at high rate loads. The specimens were failed with a sudden fracture process (sharp decrease of load after reaching the maximum value) without noticeable post-yielding phase in the curve suggesting the presence of generalized yielding (fracture patterns resembling brittle fracture). A similar failure behavior showing a sudden structural collapse was reported in Link et al.[42] and Yang.[69] Previous femur fracture FE studies were able to predict the ultimate force at fracture. Nevertheless, these studies failed to predict the complete F/U curves until complete failure. A more physical approach to determine the value of the fracture force is to consider the maximum force from the F/U curve before the drop due to propagation of the cracks.

Excellent agreement is obtained between measured and current F/U curves (Fig. 5) for different femur states (osteoporotic, osteopenic and healthy) suggesting that CDM present a suitable framework to develop accurate and robust hip fracture models.

The predicted fracture patterns for the ten specimens showed that the fracture start at the superior cortex suggesting that the entire superior surface would be more prone to failure than the inferior surface during a stance configuration for the tested femurs. Mayhew et al.[47] used QCT to demonstrate that the superior cortex was significantly thinner in older than younger individuals, while the inferior cortex was significantly thicker in older than younger individuals. In the current study, all the specimens were harvested from elderly people. Therefore, the entire superior surface would be more prone to failure than the inferior surface and would thus constitute a relatively weak region in the proximal femoral structure.

Limited number of FE studies has compared the predicted and experimentally obtained final fracture patterns.[6,12,18,35,51] Due to the nature of the uncoupled fracturing approaches applied on these works, these models were able to predict only the initial failure location but failed to predict the progressive propagation of the fracture which generate the final fracture pattern of the specimen. Keyak et al.[35] reported that the predicted fracture locations (subcapital fracture in all specimens) agreed well with the experimental ones for 13 out of 18 hip specimens under a stance configuration. However, precise correspondence of the fracture site was not provided. Bessho et al.[6] developed a CT/FE model to predict hip fracture under stance load and compared accurately the experimental fracture sites based on reconstructed CT scans of the specimens that had undergone mechanical testing. The authors compared the experimental fracture sites with the locations of the failed FE of the mesh. They applied a fracture criteria based on Drucker–Prager equivalent stress. Cristofolini et al.[12] predicted the point of
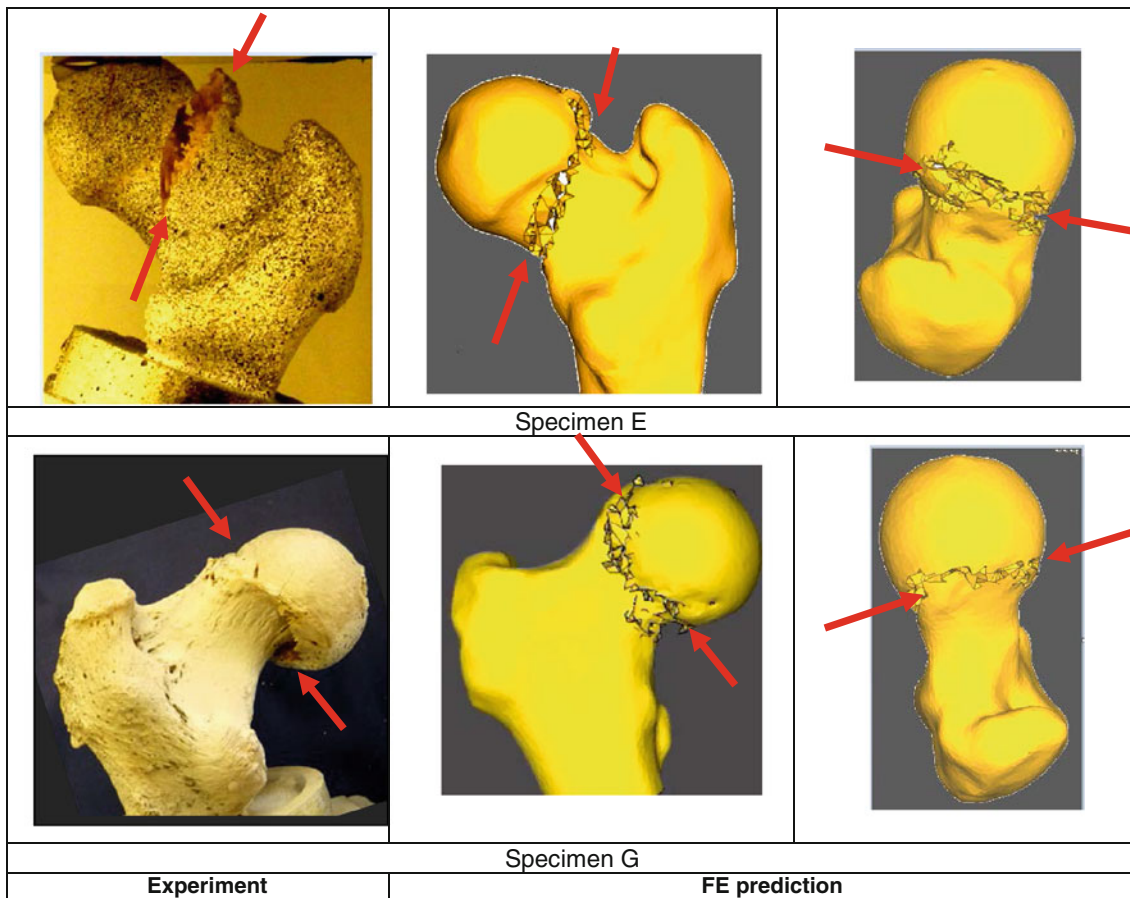
FIGURE 8. An example of experimental and FE predicted complete fracture patterns of a proximal femur (specimen G).
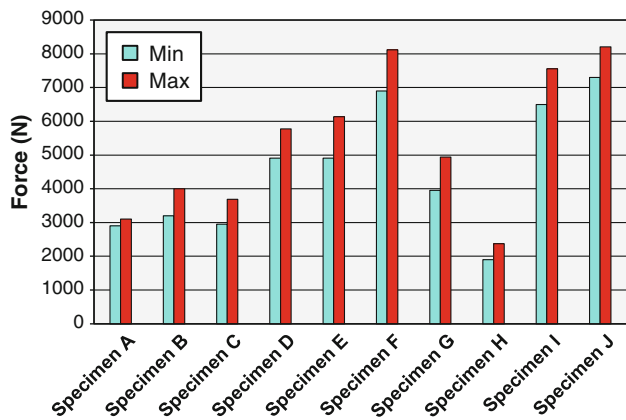

FIGURE 9. Fracture force vs. the variation of the critical damage value in compression and tension for all the specimens.

fracture initiation using a 3D FE model based on a principal strain criterion.

Although the inaccuracies related to the specimens scanning, segmentation, FE mesh generation and applied boundary conditions, excellent agreement was obtained between experimental and predicted fracture patterns indicating that proposed simple hip fracture QCT/FE model is robust and accurate to simulate human proximal femur progressive fracture until complete bone failure under quasi-static load. The model allows for the prediction of the F/U curve and the fracture pattern of the hip.

10 femur specimens were tested in stance loading conditions for validation and the predicted fracture loads and fracture profiles were compared with the experimental ones. The proposed FE model leads to excellent agreement ($R^2 = 0.9432$) between predicted and measured results concerning the shape of the F/U curve (yielding and fracturing) and the profile of the fractured edge. Most previous QCT/FE femur fracture models applied uncoupled bone fracture criteria based on local strain and/or stress components. Stress-based failure criteria are sensitive to the accuracy of the assigned material properties since the stress depends mainly on the Young modulus value. Inaccuracy of the computation of the Young modulus will generates inaccurate estimation of local applied stress. The strain based criteria overcome these problems because the strain is a kinematic measurement of the deformation alone. Nevertheless, uncoupled stress/strain fracture

criteria are not able to describe the physical damage initiation and its progressive propagation leading to complete failure because the damage variable acts as a stiffness reduction factor. For increasing damage, the effective stiffness moduli $(1 - D)C_{ijkl}$ decrease leading to the redistribution of the stress state in the vicinity of the damaged/fractured zone.

The results predicted from FE simulations in the present study should be interpreted in accordance with the limiting assumptions of the model. The first limitation of the present study is that only one loading case (stance) was investigated for and did not for the moment explore other relevant positions such as the fall on a side, which is under study. Even if most of the clinical fractures are observed after a fall,[13,26] Keyak[31] reported a strong correlation between the fracture load values in stance and lateral configurations, indicating that the load in one configuration might be a predictor of the behavior in the other position. In addition, the prediction of hip fracture in stance configuration is necessary to study the incidence of spontaneous fractures.[11,68]

The second limitation is associated with the relatively slow loading rate of 20 mm min^{-1}. The slow strain rate may generate a less pronounced brittle behavior of bone, making the damage and cracks accumulation larger compared to those obtained by applying physiological rates of about 2 mm s^{-1}.[11] FE hip fracture constitutive equations and damage law considering the strain-rate effects have to be further investigated in future research activities.

A third limitation lies in the application of the isotropic homogeneous hypothesis. It is well known that human femur is anisotropic and heterogeneous. However, the determination of anisotropic material orientations from clinical QCT scans remains an open question and is difficult to apply in the framework of daily clinical applications. In addition, several investigations showed that in the case of one-legged stance, only local differences (strains, stresses and displacement) were observed and that the whole mechanical response of the femur (fracture force and fracture location) was quite similar.[34,45,67,70]

The fourth limitation is related to the specimens' number. Only ten femoral specimens were tested in the present study. Additional work is needed with a larger samples number to perform a complete statistical analysis. However, the aim of the present study was limited to the development of a FE fracture model with experimental validation.

The fifth limitation lies in the application of the quasi-brittle model of bones without considering the material hereditariness that have been neglected since the bone preparation eliminated the water component of the bone. However, material hereditariness may be very important in presence of non-monotonic loads, as well as in crack sensitivity to the speed of load application. In this regard, several advanced model of material hereditariness may be coupled and used in conjunction with the quasi-brittle damaged one.[16,17]

These limitations do not detract from the importance of the proposed CDM based femur fracture simulation. There will still be a need to perform FE simulations to predict the fracture conditions of human proximal femurs under a given boundary risk (stance, side fall). This study exemplifies that the current CDM approach is an enhanced, practical and simple model that can be applied in clinical computer-aided decision making. Further experimental tests are needed for validation and to investigate the anisotropic mechanical behavior of human femur, as well as reliable numerical mapping methods to assign anisotropic directions and the corresponding heterogeneous material properties. Also, before potential clinical implementation, further SA and validation is needed by performing several experiments with different bone samples and boundary conditions.

From a clinical point of view, it is also important to remark that a better knowledge of the fracture mechanism and the identification of the most probable fracture region would aid to prevent them and to design better hip protectors and rehabilitation treatments.[72] A diagnostic tool that can detect osteoporotic fracture for aged patients in an early stage and predict bone strength accurately in individual patients is indispensable to prevent hip fractures.[54] The advantage of the proposed CT-based FE hip fracture model is that it could allow patient specific prediction of possibly fracture force and fracture site. Before potential clinical implementation, further validation with *ex vivo* experimental results by performing several experiments with different bone samples and boundary conditions and clinical fracture observations is needed.

CONFLICTS OF INTEREST

None.

REFERENCES

[1]Abaqus 6.11 Documentation, Analysis User's Manual.
[2]Abdel-Wahab, A. A., and V. V. Silberschmidt. Numerical modeling of impact fracture of cortical bone tissue using X-FEM. *J. Theor. Appl. Mech.* 49(3):599–619, 2011.
[3]Arthur Moore, T. L., and L. J. Gibson. Microdamage accumulation in bovine trabecular bone in uniaxial compression. *J. Biomech. Eng.* 124(1):63–71, 2002.
[4]Baca, V., Z. Horak, P. Mikulenka, and V. Dzupa. Comparison of an inhomogeneous orthotropic and isotropic material models used for FE analyses. *Med. Eng. Phys.* 30:924–930, 2008.
[5]Bayraktar, H. H., E. F. Morgan, G. L. Niebur, G. E. Morris, E. K. Wong, and T. M. Keaveny. Comparison of the elastic and yield properties of human femoral trabecular and cortical bone tissue. *J. Biomech.* 37:27–35, 2004.
[6]Bessho, M., I. Ohnishi, J. Matsuyama, T. Matsumoto, K. Imai, and K. Nakamura. Prediction of strength and strain of the proximal femur by a CT-based finite element method. *J. Biomech.* 40:1745–1753, 2007.
[7]Budyn, E., and T. Hoc. Analysis of micro fracture in human Haversian cortical bone under transverse tension using extended physical imaging. *Int. J. Numer. Methods Eng.* 82:940–965, 2010.
[8]Burr, D. B., and T. Stafford. Validity of the bulk-staining technique to separate artifactual from in vivo bone microdamage. *Clin. Orthop. Relat. Res.* 260:305–308, 1990.
[9]Chaboche, J. L. Continuum damage mechanics: a tool to describe phenomena before crack initiation. *Nucl. Eng. Des.* 64:233–247, 1981.
[10]Cotton, D. W., C. L. Whitehead, S. Vyas, C. Cooper, and E. A. Patterson. Are hip fractures caused by falling and breaking or breaking and falling? Photoelastic stress analysis. *Forensic Sci. Int.* 65:105–112, 1994.
[11]Cristofolini, L., M. Juszczyk, S. Martelli, F. Taddei, and M. Viceconti. In vitro replication of spontaneous fractures of the proximal human femur. *J. Biomech.* 40:2837–2845, 2007.
[12]Cristofolini, L., E. Schileo, M. Juszczyk, F. Taddei, S. Martelli, and M. Viceconti. Mechanical testing of bones: the positive synergy of finite-element models and in vitro experiments. *Philos. Trans. Math. Phys. Eng. Sci.* 368(1920):2725–2763, 2010.
[13]Cumming, R. G., and R. J. Klineberg. Fall frequency and characteristics and the risk of hip fracture. *J. Am. Geriatr. Soc.* 42(7):774–778, 1994.
[14]Currey, J. D. Bones: Structure and Mechanics. Princeton: Princeton University Press, 2002.
[15]Dall'Ara, E., B. Luisier, R. Schmidt, F. Kainberger, P. Zysset, and D. Pahr. A nonlinear QCT-based finite element model validation study for the human femur tested in two configurations in vitro. *Bone* 1:27–38, 2013.
[16]Di Paola, M., F. Paolo Pinnola, and M. Zingales. A discrete mechanical model of fractional hereditary materials. *Meccanica* (on line), 2013.
[17]Di Paola, M., and M. Zingales. Exact mechanical models of fractional hereditary materials. *J. Rheol.* 56:983, 2012.
[18]Dragomir-Daescu, D., J. Op Den Buijs, S. McEeligot, Y. Dai, R. C. Entwistle, C. Salas, J. Melton, III, E. Bennet,

S. Khosla, and S. Amin. Robust QCT/FEA models of proximal femur stiffness and fracture load during a sideways fall on the hip. *Ann. Biomed. Eng.* 39(2):742–755, 2011.
[19]Fritsch, A., C. Hellmich, and L. Dormieux. Ductile sliding between mineral crystals followed by rupture of collagen crosslinks: experimentally supported micromechanical explanation of bone strength. *J. Theor. Biol.* 260(2):230–252, 2009.
[20]Gassara, F., R. Hambli, T. Bouraoui, F. El Halouani, and D. Soulat. Optimization of springback in L-bending process using a coupled Abaqus/Python algorithm. *Int. J. Adv. Manuf. Technol.* 44(1/2):61–67, 2009.
[21]Hambli, R. Multiscale prediction of crack density and crack length accumulation in trabecular bone based on neural networks and finite element simulation. *Int. J. Numer. Methods Biomed. Eng.* 27(4):461–475, 2011.
[22]Hambli, R. Apparent damage accumulation in cancellous bone using neural networks. *J. Mech. Behav. Biomed. Mater.* 4(6):868–878, 2011.
[23]Hambli, R. A quasi-brittle continuum damage finite element model of the human proximal femur based on element deletion. *Med. Biol. Eng. Comput.* (Online), 2013.
[24]Hambli, R., and A. Barkaoui. Physically based 3D finite element model of a single mineralized collagen microfibril. *J. Theor. Biol.* 301:28–41, 2012.
[25]Hambli, R., A. Bettamer, and S. Allaoui. Finite element prediction of proximal femur fracture pattern based on orthotropic behaviour law coupled to quasi-brittle damage. *Med. Eng. Phys.* 34(2):202–210, 2012.
[26]Hayes, W. C., E. R. Myers, J. N. Morris, T. N. Gerhart, H. S. Yett, and L. A. Lipsitz. Impact near the hip dominates fracture risk in elderly nursing home residents who fall. *Calcif. Tissue Int.* 52(3):192–198, 1993.
[27]Hellmich, Ch., A. Dejaco, and St. Scheiner. Multiscale mechanics and mechanobiology for bone and bone tissue engineering. *J. Tissue Eng. Regen. Med.* 6(S1):389, 2012.
[28]Juszczyk, M. M., L. Cristofolini, and M. Viceconti. The human proximal femur behaves linearly elastic up to failure under physiological loading conditions. *J. Biomech.* 44(12):2259–2266, 2011.
[29]Kaneko, T. S., M. R. Pejcic, J. Tehranzadeh, and J. H. Keyak. Relationships between material properties and CT scan data of cortical bone with and without metastatic lesions. *Med. Eng. Phys.* 25(6):445–454, 2003.
[30]Keaveny, T. M., E. F. Wachtel, and D. L. Kopperdahl. Mechanical behavior of human trabecular bone after overloading. *J. Orthop. Res.* 17:346–353, 1999.
[31]Keyak, J. H. Relationships between femoral fracture loads for two load configurations". *J. Biomech.* 33(4):499–502, 2000.
[32]Keyak, J. H. Improved prediction of proximal femoral fracture load using nonlinear finite element models. *Med. Eng. Phys.* 23:165–173, 2001.
[33]Keyak, J. H., and Y. Falkinstein. Comparison of in situ and in vitro CT scan-based finite element model predictions of proximal femoral fracture load. *Med. Eng. Phys.* 25:781–787, 2003.
[34]Keyak, J., J. Meagher, H. Skinner, and J. Mote. Automated three-dimensional finite element modelling of bone: a new method. *ASME J. Biomech. Eng.* 12:389–397, 1990.
[35]Keyak, J. H., S. A. Rossi, K. A. Jones, C. M. Les, and H. B. Skinner. Prediction of fracture location in the proximal femur using finite element models. *Med. Eng. Phys.* 23:657–664, 2001.

[36]Keyak, J. H., S. A. Rossi, K. A. Jones, and H. B. Skinner. Prediction of femoral fracture load using automated finite element modeling. *J. Biomech.* 31:125–133, 1998.

[37]Keyak, J. H., and H. B. Skinner. Three-dimensional finite element modelling of bone: effects of element size. *J. Biomed. Eng.* 14:483–489, 1992.

[38]Koivumäki, J. E., J. Thevenot, P. Pulkkinen, V. Kuhn, T. M. Link, F. Eckstein, and T. Jämsä. Ct-based finite element models can be used to estimate experimentally measured failure loads in the proximal femur. *Bone* 50(4):824–829, 2012.

[39]Kotha, S. P., and N. Guzelsu. Tensile damage and its effects on cortical bone. *J. Biomech.* 36(11):1683–1689, 2003.

[40]Lakes, R. S. Materials with structural hierarchy. *Nature* 361:511–515, 1993.

[41]Lemaitre, J. A continuous damage mechanics model for ductile fracture. *J. Eng. Mater. Technol.* 107:83–89, 1985.

[42]Link, M., V. Vieth, R. Langenberg, N. Meier, A. Lotter, D. Newitt, and S. Majumdar. Structure analysis of high resolution magnetic resonance imaging of the proximal femur: in vitro correlation with biomechanical strength and BMD. *Calc. Tissue Int.* 72:156–165, 2003.

[43]Lotz, J. C., E. J. Cheal, and W. C. Hayes. Fracture prediction for the proximal femur using finite element models. Part I. Linear analysis. *J. Biomech. Eng.* 113:353–360, 1991.

[44]Malik, L., M. Stover, B. Martin, and C. Gibeling. Equine cortical bone exhibits rising R-curve fracture mechanics. *J. Biomech.* 36:191–198, 2003.

[45]Martelli, S., F. Taddei, E. Varini, L. Cristofolini, L. Gill, and M. Viceconti. Accuracy of subject specific finite-element models of long bones from CT data: an in vitro study. *Proc. ICCB II* 1:251–265, 2005.

[46]Martin, R. B., and D. B. Burr. Structure, Function, and Adaptation of Compact Bone. New York: Raven, 1989.

[47]Mayhew, P. M., C. D. Thomas, J. G. Clement, N. Loveridge, T. J. Beck, W. Bonfield, C. J. Burgoyne, and J. Reeve. Relation between age, femoral neck cortical stability, and hip fracture risk. *Lancet* 366:129–135, 2005.

[48]Mazars, J., and G. Pijaudier-Cabot. From Damage to fracture mechanics and conversely: a combined approach. *Int. J. Solid Struct.* 33:3327–3342, 1996.

[49]Murakami, S., and Y. Liu. Mesh-dependence in local approach to creep fracture. *Int. J. Damage Mech* 4:230–250, 1995.

[50]Nagaraja, S., T. L. Couse, and R. E. Guldberg. Trabecular bone microdamage and microstructural stresses under uniaxial compression. *J. Biomech.* 38:707–716, 2005.

[51]Ota, T., I. Yamamoto, and R. Morita. Fracture simulation of femoral bone using finite-element method: how a fracture initiates and proceeds. *J. Bone Miner. Metab.* 17(2):108–112, 1999.

[52]Pattin, C. A., W. E. Caler, and D. R. Carter. Cyclic mechanical property degradation during fatigue loading of cortical bone. *J. Biomech.* 29:69–79, 1996.

[53]Peng, L., J. Bai, X. Zeng, and Y. Zhou. Comparison of isotropic and orthotropic material property assignments on femoral finite element models under two loading conditions. *Med. Eng. Phys.* 28:227–233, 2006.

[54]Ray, N. F., J. K. Chan, M. Thamer, and L. J. Melton. Medical Expenditures for Treatment of Osteoporosis Fractures in the United States in 1995: report From the National Osteoporosis Foundation. *J. Bone Miner. Res.* 12:24–25, 1997.

[55]Reilly, D. T., and A. H. Burstein. The elastic and ultimate properties of compact bone tissue. *J. Biomech.* 8:393–405, 1975.

[56]San Antonio, T., M. Ciaccia, C. Müller-Karger, and E. Casanova. Orientation of orthotropic material properties in a femur FE model: a method based on the principal stresses directions. *Med. Eng. Phys.* 34(7):914–919, 2012.

[57]Schileo, E., F. Taddei, L. Cristofolini, and M. Viceconti. Subject-specific finite element models implementing a maximum principal strain criterion are able to estimate failure risk and fracture location on human femurs tested in vitro. *J. Biomech.* 41(2):356–367, 2008.

[58]Schileo, E., F. Taddei, A. Malandrino, L. Cristofolini, and M. Viceconti. Subject-specific finite element models can accurately predict strain levels in long bones. *J. Biomech.* 40:2982–2989, 2007.

[59]Smith, M. D., D. D. Cody, A. M. Cooperman, S. A. Goldstein, L. S. Matthews, and M. J. Flynn. Proximal femur bone density and its correlation to fracture load and hip screw penetration load. *Clin. Orthop. Relat. Res.* 283:244–251, 1992.

[60]Sobelman, O. S., J. C. Gibeling, S. M. Stover, S. J. Hazelwood, O. C. Yeh, D. R. Shelton, and R. B. Martin. Do microcracks decrease or increase fatigue resistance in cortical bone? *J. Biomech.* 37(9):1295–1303, 2004.

[61]Taylor, D., and T. C. Lee. A crack growth model for the simulation of fatigue in bone. *Int. J. Fatigue* 2:387–395, 2003.

[62]Tellache, M., M. Pithioux, P. Chabrand, and C. Hochard. Femoral neck fracture prediction by anisotropic yield criteria. *Eur. J. Comput. Mech.* 18(1):33–41, 2009.

[63]Trabelsi, N., Z. Yosibash, and C. Milgrom. Validation of subject-specific automated p-FE analysis of the proximal femur. *J. Biomech.* 42:234–241, 2009.

[64]Turner, C. H. Bone strength: current concepts. *Ann. N. Y. Acad. Sci.* 1068:429–446, 2006.

[65]Ural, A., and D. Vashishth. Anisotropy of age-related toughness loss in human cortical bone: a finite element study. *J. Biomech.* 40:1606–1614, 2007.

[66]Vashishth, D., E. Tanner, and W. Bonfield. Experimental validation of a microcracking-based toughening mechanism for cortical bone. *J. Biomech.* 36(1):121–124, 2003.

[67]Verhulp, E., B. van Rietbergen, and R. Huiskes. Comparison of micro-level and continuum level voxel models of the proximal femur. *J. Biomech.* 39:2951–2957, 2006.

[68]Viceconti, M., F. Taddei, L. Cristofolini, S. Martelli, C. Falcinelli, and E. Schileo. Are spontaneous fractures possible? An example of clinical application for personalised, multiscale neuro-musculo-skeletal modelling. *J. Biomech.* 45:421–426, 2012.

[69]Yang, H., L. Shen, K. Demetropoulos, I. King, P. Kolodziej, S. Levine, and J. Fitzgerald. The relationship between loading conditions and fracture patterns of the proximal femur. *J. Biomech. Eng.* 118:575–578, 1996.

[70]Yosibash, Z., D. Tal, and N. Trabelsi. Inhomogeneous orthotropic material properties high-order finite-element analysis with inhomogeneous orthotropic material properties. *Philos. Trans. R. Soc. A* 368:2707–2723, 2010.

[71]Zimmermann, E. A., H. D. Barth, and R. O. Ritchie. The multiscale origins of fracture resistance in human bone and its biological degradation. *JOM* 64(4):486–493, 2012.

[72]Zuckerman, J. D. Hip fracture. *N. Engl. J. Med.* 334:1519–1525, 1996.